

In-vitro and In-vivo Characterization of Silica Nanoparticles for the Treatment of Liver Cancer

Anurima Singh¹, Laxmikant Sahu², Kamini Verma*³, Niharika Dewangan³

¹Rungta Institute of Pharmaceutical Education and Research, Kohka – 490024, Bhilai, Chhattisgarh, India

²Rungta Institute of Pharmaceutical Sciences and Research, Kohka – 490024, Bhilai, Chhattisgarh, India

³Department of Life Science, Shri Shankaracharya Professional University, Junwani - 490020, Bhilai, Chhattisgarh, India

*Corresponding author

Kamini Verma

Shri Shankaracharya Professional University, Junwani - 490020, Bhilai, Chhattisgarh, India

Abstract:

In the present study, we successfully developed a preferable doxorubicin (Dox) loaded drug delivery system

based on Cetuximab and silica nanoparticles. By employing the tumor homing property of Cetuximab and the drug-loading capability of silica nanoparticles, the prepared Cet-SLN/Dox was able to load Dox to achieve the co-delivery of two drugs. In vitro analysis revealed that Cet-SLN/Dox was nano-sized particles with decent drug loading capabilities and smart drug release profile. Further studies demonstrated that Cet-SLN/Dox was superior in tumor-homing and anti-cancer efficiency than Cetuximab free SLN/Dox and free Dox, possibly due to EGFR mediated endocytosis and the combined anti-cancer effects of Cetuximab and Dox within Cet-SLN/Dox.

Keywords: Silica nanoparticles; *In-vitro* study; *In-vivo* study; Doxorubicin; Liver cancer therapy

1. Introduction

Liver cancer is globally the sixth most frequent cancer, and the second leading cause of cancer death, which is responsible to 746,000 deaths in 2012 alone. According to the World Cancer Report in 2014, liver cancer has a low five year survival rates of 17% in the United States alone and merely 4.6% worldwide [1]. To date, various drug delivery systems (DDS) have been successfully been developed toward increasing therapeutic efficiency of liver cancer on the basis of diverse materials ranging from organic ones to inorganic ones, including polymeric micelles lipid carriers polyplexes calcium carbonate gold, silica and titanium dioxide nanoparticles [2]. Among all these potential candidates, silica nanoparticles with preferable characteristics such as ease of synthesis and modification, high drug loading efficiency and low cytotoxicity, has made it a well-recognized biomaterial in drug delivery and cancer therapy, of which many desirable formulations have been designed based on silica nanoparticles [3]. However, until now, only few drug delivery vectors can finally achieve the required therapeutic effect since most of them fail to effectively targeting the cancer site and terminating the cancer cells. As a result, drug delivery vectors conjugated with various targeting ligands have been developed to enhance the accumulation of nanoparticles within the tumor site and reduce the unwanted side effects [4]. Despite that various cancer therapy approaches are available, chemotherapy remains to the most important and indispensable one under the current situation. In recent years, monoclonal antibodies which can specifically recognize and bind to the over-expressed corresponding receptors on cancer cells are treated as a promising chemotherapy candidate for cancer therapy. Moreover, it has been well-documented that combination chemotherapy using two or more drugs can achieve better therapeutic effect than applying any one of the drugs alone, since they can exert beneficial effect on cancer cells by regulating different pathways [5]. Cetuximab is a monoclonal antibody that binds to epidermal growth factor receptor (EGFR) and inhibits its epidermal growth factor signaling within cancer cells, its potential application in liver cancer therapy has been proposed and proved to be positive [6]. Doxorubicin as a broad-spectrum anti-cancer drug, is commonly used in the treatment of a wide range of cancers, including liver cancer. On the other hand, Dox also adopted in combination chemotherapy as a component of various chemotherapy regimens. Herein we seek to explore the possibility of enhanced liver cancer therapy using combination chemotherapy of Cetuximab and Dox [7]. To finally achieve the combination chemotherapy of Cetuximab and Dox, while at the same time, rendering the vector tumor targeting ability, proper designs should be proposed. In our study, thiolated SLNs were firstly synthesized and then conjugated with thiolated Cetuximab to construct the tumor-targeting and tumor

microenvironment responsive system (Cet-SLNs). Finally, the as prepared Cet-SLNs were subjected to drug loading of Dox to fulfill the binary drug delivery purpose (Cet-SLN/Dox) [8]. We hope to employ the high tumor-homing property of Cetuximab to specifically guide the Cet-SLN/Dox to the cancer site and further, increase its cellular uptake efficiency. Once the Cet-SLN/ Dox is accumulated within the cancer cells, the exceptional high concentration of glutathione in the cytoplasm will therefore trigger the release of Cetuximab, which can finally exert combinational anti-cancer effect with Dox [9].

2. Materials and methods

Triton X-100, tetraethyl orthosilicate (TEOS), (3-mercaptopropyl)-trimethoxysilane (MPTMS) and β -mercaptoethylamine (MEA) were obtained from the Sigma Aldrich, Mumbai, Maharashtra, India. Doxorubicin hydrochloride (Dox) was supplied by Loba Chemie Mumbai, Maharashtra, India. Cetuximab was purchased from Merck Mumbai, Maharashtra, India. Glutathione (GSH), 3-(4,5-dimethylthiazol-2-yl)-2,5-diphenyl tetrazolium bromide (MTT), DiR iodide (DiR) and Hoechst 33342 were purchased from Sigma-Aldrich Mumbai, Maharashtra, India. All other chemicals and reagents were purchased from Loba Chemie Mumbai, Maharashtra, India.

Cell culture and animal model

The human hepatocellular liver carcinoma cell line (HepG2) purchased from American Type Culture Collection (ATCC, Manassas, VA, USA) was maintained in Dulbecco minimum essential medium supplemented with 10% (v/v) heat-inactivated fetal bovine serum, 2 mM glutamine, 10 mM 4-(2-hydroxyethyl)-1-piperazineethanesulfonic acid buffer, 100 U/mL penicillin and streptomycin at 37 °C in a humid atmosphere (5% CO₂, 95% air). Male Balb/c nude mice (20 g), which obtained from Suzhou Belda Bio-Pharmaceutical Co., Ltd. were housed in at strict temperature-controlled (25 ± 2 °C) SPF-II house with enough food and water. To generate the HepG2 cancer model, HepG2 cells with concentration of 5 × 10⁷ cells/mL in saline were subcutaneously injected into the flank of each Balb/c nude mouse (100 μ L per mouse). The mice were applied to in-vivo experiments when the tumor volumes approached about 100 mm³.

Preparation of Cet-SLN/Dox

Thiolated SLN was firstly synthesized in a water-in-oil microemulsion with minor modification as previously reported [10]. Briefly, a water-in-oil microemulsion was prepared by mixing 1.8 mL Triton X-100, 7.5 mL cyclohexane, 1.6 mL n-hexanol, and 480 μ L of water. After stirring for 0.5 h, 180 μ L TEOS and 60 μ L MPTMS were then added as precursors for silica matrix formation, followed by the

addition of 100 μL NH_4OH to initiate the polymerization process. The reaction was allowed to continue for 24 h at room temperature. After the reaction was completed, the thiol-functionalized SLNs were precipitated by addition of ethanol and were washed with ethanol and water respectively for several times to remove the excess surfactant molecules from the particles. Thiolated Cetuximab was prepared according to previous reported method [11]. In brief, Cetuximab (1 mg) was thiolated by reacting with MEA in degassed phosphate buffered saline (PBS, pH 7.4) for 90 min at 37 $^\circ\text{C}$. The Cetuximab was then purified by ultrafiltration in an Amicon cell (MW = 10 kDa). 500 μg of thiolated Cetuximab was added into the aqueous solution of thiolated SLN (1 mg/mL, 5 mL) and co-incubated with gentle agitation at room temperature for 6 h. Finally, the Cet-SLNs were isolated from the solution under high speed of centrifugation (8000 $\times g$ for 10 min, CR21, Hitachi, Japan). Standard protocol of Bradford assay was employed for quantifying the concentration of the Cetuximab in the supernatant to determine the surface density of Cetuximab as previous reported [19]. The amount of the ligand conjugated on the SLN surface was obtained via reduction of the amount in the supernatant from the initial amount. Briefly, 50 μL of the solution was mixed with 1.5 mL Bradford reagent and incubated for 15 min before measuring absorption at 590 nm using a UV-Vis spectrophotometer. The as prepared Cet-SLNs were resuspended in 3 mL deionized water and stirred for 1 h to ensure complete dispersion. On the other hand, DOX was dissolved in DMF in the presence of TEA (molar ratio of TEA: DOX = 1.5:1). Afterwards, the DOX solution was dropwise added into Cet-SLNs solution with vigorous agitation, followed by sonication with a probetype ultrasonicator at 100 W for 30 min. The mixture was centrifuged at 8000 $\times g$ for 10 min to isolate the Cet-SLN/Dox. The supernatant was collected and subjected to fluorescence measurement to calculate the drug loading efficiency of Cet-SLN/Dox. The excitation wavelength, emission wavelength and slit openings were set at 505, 565, and 5 nm, respectively. Drug loading content (DLC) was calculated according to the following formula:

$$\text{DLC (wt\%)} = (\text{weight of loaded Dox} / \text{weight of Cet-SLN/Dox}) \times 100\%$$

To further confirm that Cetuximab was linked to the SLNs, fluorescence investigation was performed as previous reported [12]. Briefly, 2 μL fluorescein isothiocyanate (FITC)-conjugated rabbit-anti-human IgG was added to 100 μL of Cet-SLN/Dox (1:50, v/v) with 0.9% bovine serum albumin and allowed to incubate at room temperature for 1 h. After centrifugation at 8000 $\times g$ for 10 min, the precipitate was washed three times with phosphate buffer saline (PBS), redispersed in 20 μL of PBS and observed under an inverted fluorescence microscope [13].

Particle size and morphology observation

The size distributions, mean particle size and polydispersity index (PDI) of different nanoparticles were assessed by dynamic light scattering (DLS) method using zeta plus zeta potential analyzer at 25 °C. For morphology observation, a single drop of each solution was deposited on a transmission electron microscope (TEM) grid and allowed to air dry. All samples were imaged using a JEM-200CX TEM with an acceleration voltage of 80 kV.

In vitro release experiments

The responsive release of Cetuximab and Dox from Cet-SLN/Dox was investigated by centrifugation method. Cet-SLN/Dox were suspended in PBS (pH 7.4, containing 0.1% Tween 80, w/v), to which GSH was added to achieve 2 mM (extracellular level) and 10 mM (intracellular level), respectively. At predetermined time intervals, the solution was centrifuged at 8000 ×g for 10 min and the supernatant was measured by its absorption value at 590 nm using a UV–Vis spectrophotometer for Cetuximab release. Besides, the comparative release behaviour of Dox from Cet-SLN/Dox under different conditions was further determined by fluorescence spectrophotometer at excitation wavelength, emission wavelength and slit openings set at 505, 565, and 5 nm, respectively.

Cytotoxicity activity

To study the cytotoxicity of free nanoparticles and Cet-SLN/Dox, the harvested individual HepG2 cells were seeded (96-well plates) overnight to reach confluence of 70–80%. After that, cells were incubated for 48 h in the presence of different samples: free Dox, drug free thiolated SLNs, Dox free Cet-SLNs and Cet-SLN/Dox (Dox concentration was set at 0.25, 0.5, 1.25, 2.5, 7.5 µg/mL). After proper incubation, standard MTT assay was applied to evaluate the cell viability of all tested samples [14-15].

Cellular uptake of Cet-SLN/Dox

The internalization profile of SLN/Dox and Cet-SLN/Dox in HepG2 cell line was assessed by monitoring the innate fluorescence signal of Dox. HepG2 cells with a density of 1×10^5 cells/dish were seeded in confocal dishes ($\Phi = 15$ mm) and cultured for another 12 h. Then cells were treated with 1 mL of the serum-free medium containing SLN/ Dox and Cet-SLN/Dox after discarding the previous culture medium. To confirm that Cet-SLN/Dox was taken up through Cetuximab related endocytosis, cells were further incubated with 100 µg/mL Cetuximab solution for 2 h prior to nanoparticles addition. After 2, 4 and 6 h of incubation, the cells were treated with Hoechst 33342 (10 µg/mL) for 15 min and rinsed three

times with PBS before qualitatively imaged by confocal laser scanning microscopy. For quantitative determination of the fluorescence intensity of each group, the culture media were discarded, cells were harvested and subjected to flow cytometer (FCM, BD FACSCalibur™, USA, excitation was conducted with a 485 nm argon laser, and the fluorescence emission at 595 nm was measured, a minimum of 1×10^4 cells from each sample were randomly selected for measurement).

In vivo distribution of Cet-SLN/DiR nanoparticles

Near infrared fluorescent (NIR) probe DiR was encapsulated in the nanoparticles in the same protocol as for the Dox loading (Cet-SLN/ DiR). The HepG2 tumor-bearing mice were injected in the tail vein with Cet-SLN/DiR (as the experimental group) and SLN/DiR (as the control group), respectively (at a concentration of 1.0 mg/mL, 200 μ L). The in vivo tumor targeting efficacy and biodistribution of different nanoparticles at pre-determined time intervals were evaluated using In-vivo Imaging System equipped with DiR filter sets (excitation/emission, 720/790 nm). To further confirm the EGFR-mediated targeting capability of Cet-SLN/DiR, mice were firstly pretreated with Cetuximab (5 mg/kg) for 1 h and then subjected to Cet-SLN/DiR injection and in vivo imaging as mentioned above. After living imaging, the mice were sacrificed, and the tumor tissues as well as major organs (heart, liver, spleen, lung and kidney) were excised for ex vivo imaging using the same imaging system.

In vivo antitumor efficacy

The in vivo antitumor efficacy of Cet-SLN/Dox was further confirmed by employing HepG2 tumor xenograft models. All mice were divided into 5 groups (n = 5) randomly: 1) saline (control); 2) free Dox; 3) SLN/Dox; 4) Cetuximab; 5) Cet-SLN/Dox. Protocols were in accordance with previous report [16]. Briefly, all the mice were administrated via tail vein (5 mg/kg Dox and/or Cetuximab per mouse) and the administration was then repeated for 7 times in a therapeutic period of 14- days. The body weights of mice and tumor sizes were recorded before injection every other day. After the last injections, two of the mice in each group were randomly picked and sacrificed, the tumor tissues were treated with hematoxylin and eosin (HE) staining and pictured by microscope [17].

3. Results and discussions

Particle size, dispersity, morphology and drug loading of Cet-SLN/Dox

The particle size and dispersity of thiol-functionalized SLNs and CetSLN/Dox were firstly measured by dynamic light scattering technic. As shown in Fig. 1A, the thiol-functionalized SLNs obtained by water-in-oil microemulsion method were spherical, with a diameter of around 97.3 nm. Moreover, the as

prepared thiol-functionalized SLNs displayed a relatively small polydispersion index (PDI) of 0.214. This was attributed to the well-formed water pools in the microemulsion which are believed to play an important role in controlling the size and dispersity of the generated particles [18-19]. Compared with the particle size of thiol-functionalized SLNs, Cet-SLNs demonstrated a slightly increased size of around 135 nm, which might be due to the anchoring of Cetuximab on the surface of SLNs. At the same time, it was observed that the PDI (0.113) of the obtained Cet-SLNs (Fig. 1B) is lower than that of thiol-functionalized SLNs, indicating that surface modification of hydrophilic Cetuximab might be beneficial to the dispersion of CetSLNs. To further confirm the successful modification of Cetuximab on the surface of thiol-functionalized SLNs, TEM was applied to observe the morphology of thiol-functionalized SLNs and Cet-SLNs. It was shown in the inserted image in Fig. 1A that thiol-functionalized SLNs were individual particles with evident boundary to one another. However, it was also observed that some neighbouring thiol-functionalized SLNs were connected with each other, which might be due to the reaction of surface thiol groups among closely existed thiol-functionalized SLNs [20-21]. In contrast, the interparticle distance of Cet-SLNs increased compared with that of the thiol-functionalized SLNs, this is in accordance with the decreased PDI in dispersity test (Fig. 1B). On the other hand, the edges of the Cet-SLNs were relatively vague, with apparent coreshell core-structure being observed, which was believed to be the presence of Cetuximab. Besides from the particle size analyzation and morphology observation, the comparative fourier transform infrared spectrometer (FTIR) spectrum [22] of Cetuximab (upper) and Cet-SLN (lower) were also recorded in Fig. 1C. As it can be observed that the characteristics FTIR peaks in Cetuximab can also be seen in that of Cet-SLN. Fluorescent staining method was also adopted to verify the successful conjugation of Cetuximab. Dox loaded Cet-SLN/Dox and SLN/Dox was firstly incubated and then being centrifuged. After being treated by these procedures, it was expected that the Cet-SLN/Dox might aggregated to larger particles to a micrometer scale or above. Nanoparticles on such a large scale could thus be observed by fluorescence microscopy [23]. As expected from the morphology observation results, both red (from Dox) and the green (from FITC) fluorescence could observed from the CetSLN/Dox. On the contrary, only red fluorescence can be detected in Cet-free SLN/Dox (Fig. 1C). These results demonstrate that not only the Cet-SLN/Dox was successfully prepared between the thiol groups of single chain antibodies and the thiol-functionalized SLNs, but also implies that the thiolation of the antibody does not affect its bioactivity since Cet-SLN/Dox can bind with the IgG second antibody [24]. All the above results confirmed the successful modification of Cetuximab to the surface of thiol-functionalized SLNs,

resulting in the formation of Cet-SLN/Dox. The conjugation of Cetuximab on Cet-SLNs was calculated to be 15.32%. The DLC of Dox in Cet-SLN/Dox calculated by fluorescence spectrophotometer was 9.7%.

In-vitro drug release

One fatal drawback of some current existing drug delivery systems is that they are not capable of achieving selective drug release inside tumor cells, which lead to severe side effect on in vivo application. The Cet-SLN/Dox were designed to achieve dual-responsive drug release profile: one is ligand exchange in response to high concentration of GSH within tumor cells to specifically release Cetuximab, another is the subsequent facilitated release of the encapsulated Dox due to the departure of the surface Cetuximab. It was expected that, drug release profile of Cet-SLN/Dox could allow for the needs that Cetuximab and Dox molecules remained stable and unreleased under physiological environment (i.e., in the blood stream), and accelerated Cetuximab and Dox release can be achieved at tumor sites or within cancer cells. To verify the redox sensitive release behaviour of Cetuximab and Dox from Cet-SLN/Dox, Cet-SLN/ Dox were tested in different conditions: GSH solution with concentrations of 10 mM and 2 mM (mimicking the intracellular and extracellular GSH concentration, respectively). The Cetuximab and Dox release behaviors of Cet-SLN/Dox were summarized in Fig. 1D. It was concluded that Cet-SLN/Dox were stable under extracellular physiological environment, as supported by the fact that Cetuximab and Dox in were remained stable under 2 mM of GSH (extracellular GSH concentration). However, increased released can be obtained both for Cetuximab and Dox with the presence of high concentration of GSH (10 mM). It was worth noting that the release behaviour of Cetuximab and Dox demonstrated a synchronous profile. That is, the slow release of Cetuximab corresponds to slow Dox release, however, once the release of Cetuximab increased, the Dox release from Cet-SLN/Dox was also elevated.

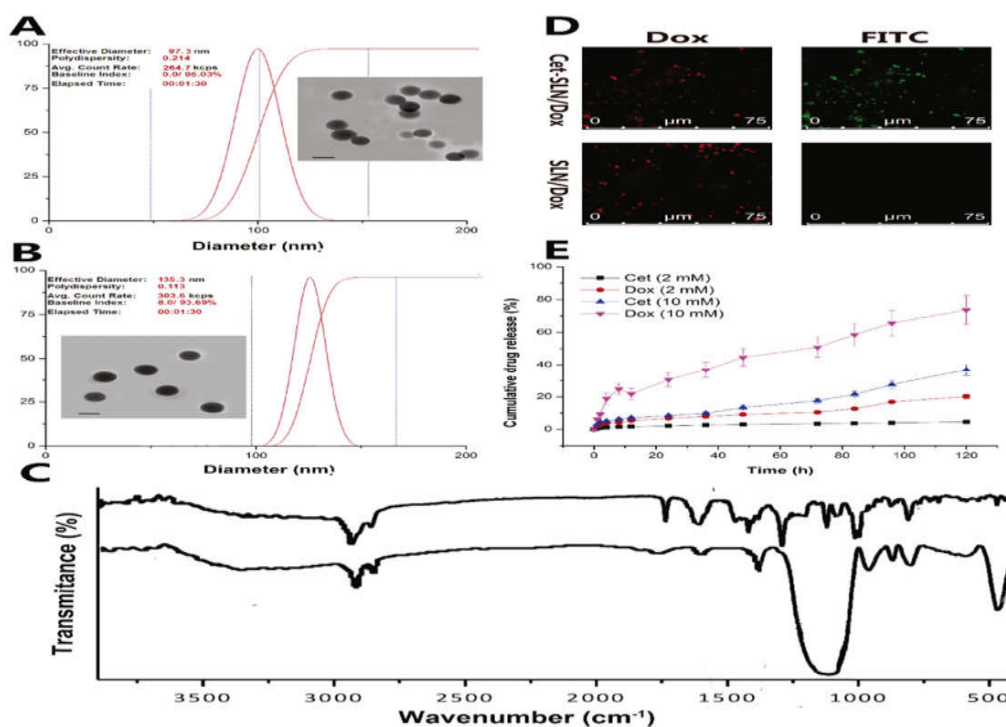


Fig.1. The size distributions, mean particle size and PDI of (A) thiol-functionalized SLNs and (B) Cet-SLN/Dox. Inserted images were morphology of corresponding nanoparticles. Scale bar: 100 nm. (C) Comparative FTIR spectrum of Cetuximab (upper) and Cet-SLN (lower). (D) Determination of antibodies on the surface of SLNs. (E) Drug release profiles of Cetuximab and Dox from the Cet-SLN/Dox in release media with intracellular and extracellular concentration of GSH (10 mM and 2 mM, respectively). Data were shown as mean \pm S.D. (n = 3)

The mechanism of GSH-induced drug release from Cet-SLN/Dox was related to the thiol group exchange reaction, in which GSH functions as a reducing agent to exchange the Cetuximab from the surface of the SLNs. On the other hand, the departure of surrounding Cetuximab on the surface of Cet-SLN/Dox might also facilitate diffusion of the internal Dox. All the above mentioned results provided several clues that Cet-SLN/Dox can achieve targeted drug release in a synergistic manner. The drug release mechanism is dependent on high GSH concentration-dependent ligand exchange reactions. The responsive drug release mechanisms permits the rapid transformation of Cet SLN/Dox into Cetuximab and Dox inside tumor cells, which is beneficial to tumor cell inhibition.

Cytotoxicity assay

In order to further explore and verify the *in vitro* Cetuximab and Dox delivery efficiency and anticancer efficiency of the well-designed Cet-SLN/Dox, MTT assay was employed to evaluate the cell viability of all tested groups. Cytotoxicity data estimated by MTT assay were displayed in Fig. 2. Prior to

formulation cytotoxicity tests, cytotoxicity test of the drug free thiolated SLNs was also conducted (nanoparticle concentrations range from 5 to 100 $\mu\text{g}/\text{mL}$, Fig. 2A) to exclude any error induced by carriers in the in vitro anticancer efficiency tests. When treated by drug free thiolated SLNs, more than 90% of the cells survived at the highest dose. The low cytotoxicity of drug free thiolated SLNs thus grant a broad range of potential application of drug free thiolated SLNs based nanoparticles in the field of cancer therapy and other biomedical utility. The anti-cancer efficacy of free Cetuximab was also conducted. It was demonstrated that free Cetuximab showed certain anti-cancer efficacy itself. The following anticancer assay with Cetuximab conjugated nanoparticles showed some interesting results. Compared with drug free thiolated SLNs, Dox free CetSLNs showed comparative anti-cancer efficacy to that of free Cetuximab at the same Cetuximab concentrations, indicating that the Cetuximab conjugated onto Cet-SLNs can still exert its anticancer effect, possibly via the responsive release of Cetuximab within cancer cells. As displayed in Fig. 2B, Cet-SLN/Dox showed much more potent anti-cancer effect than SLN/Dox at all Dox concentrations. Moreover, it was worth mentioning that Cet-SLN/Dox exhibited comparable cytotoxicity to that of free Dox at low Dox concentrations and even more increased cytotoxicity than free Dox at high Dox concentrations, implying that combined chemotherapy of Cetuximab and Dox hold stronger anticancer efficiency than either Cetuximab or Dox alone. Results also implied that with growing concentrations of Cetuximab and Dox, corresponding lethality also increased, suggesting that in vitro anticancer effect of Cet-SLN/Dox was dose-dependent (Fig. 2B). On the other hand, it was also suggested that the superior anticancer efficiency of CetSLN/Dox might be related to the improved nanoparticle internalization mediated by Cetuximab, as a proof of concept, in vitro cellular uptake experiments were performed.

Cellular uptake of Cet-SLN/Dox

It has been demonstrated by many previous articles that Cetuximab conjugated toward the surface of the DDS can target EGFR, which excessively expressed in various cancer cells, including liver cancer [19, 23, 24]. As a proof of our suggestions, Dox, as both a model drug and fluorescent molecule, was utilized as an indicator to qualitative and quantitative analyze the uptake behaviour of different samples by FCM at different time points. As shown in Fig. 2C and D, higher Dox fluorescence signals were observed in the cells of Cet-SLN/Dox group, rather than that of SLN/ Dox, as revealed by CLSM observation. It was also calculated from the FCM data that the fluorescence intensity of Cet-SLN/Dox was approximately 3.61- fold higher than that of free SLN/Dox after incubation for 6 h, suggesting that Cet-SLN/Dox can be readily internalized by HepG2 cells than its counterpart SLN/Dox, possibly via the EGFR mediated

endocytosis pathway. After Cetuximab pretreatment, a great decline in fluorescence intensity of Cet-SLN/Dox group was observed at all-time intervals while the fluorescence intensity of SLN/ Dox group still stayed at the same level. These results clearly include that Cet-SLN/Dox were internalized into cells, via EGFR-mediated endocytosis.

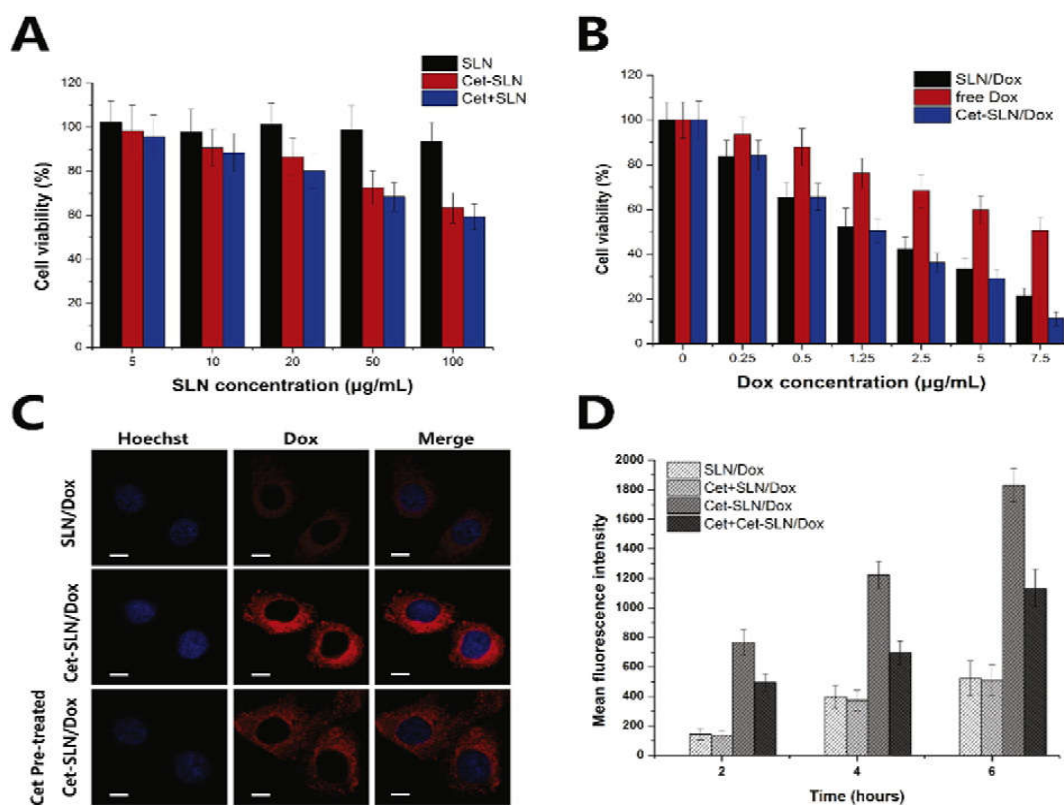


Fig.2. (A) Cytotoxicity of thiol-functionalized SLNs, Cet-SLNs and free Cetuximab plus SLNs (at the same Cetuximab concentrations) after 48 h incubation with HepG2 cells. (B) Cytotoxicity of free Dox, SLN/Dox and Cet-SLN/Dox against HepG2 cells after 48 h incubation. Data were expressed as mean \pm S.D. (n = 5). (C) Cellular uptake of SLN/Dox and Cet-SLN/Dox with and without pretreatment with free Cetuximab in HepG2 cells at 2 h post incubation at 37 °C. (D) Quantitative flow cytometric analysis of the intracellular uptake of SLN/Dox and Cet-SLN/Dox with and without Cetuximab pretreatment in HepG2 cells for 2, 4, and 6 h of incubation. Data were expressed as mean \pm S.D. (n = 3). Scale bar: 20 μ m.

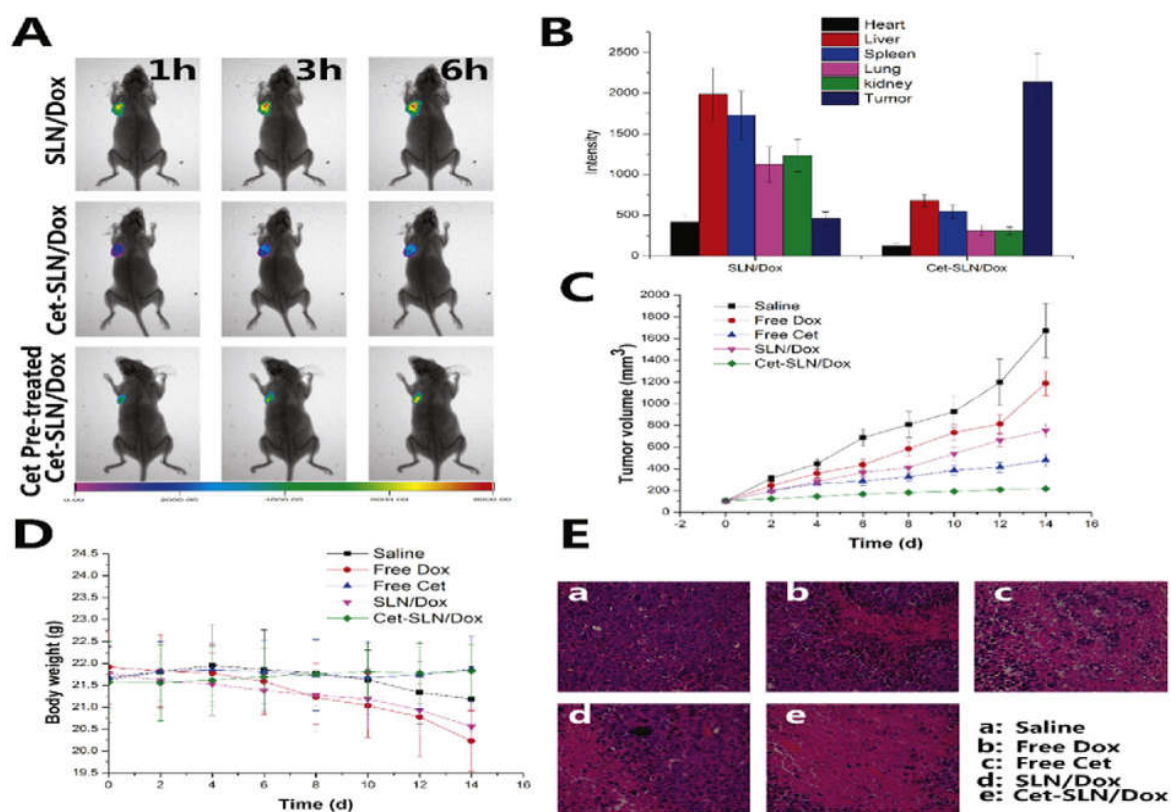


Fig.3. (A) In vivo time-dependent tumor-targeting images after intravenous injection of SLN/DiR and Cet-SLN/DiR in HepG2 tumor-bearing mice and (B) representative ex vivo mean fluorescence intensity of dissected tumors and major organs at 6 h post-injection. The tumor volume (C), body weight (D) and HE staining of tumor tissue (E) analysis of HepG2 tumor-bearing BALB/c nude mice after intravenous injection administration of saline, free Dox, free Cetuximab, SLN/Dox and Cet-SLN/Dox, respectively. The measurement of tumor volumes and the injection of formulations were repeated every 2 days for two weeks. Dose: 5 mg/kg Cetuximab and/or Dox per mouse.

In addition, the fluorescence signal demonstrated a gradually increased profile with extended incubation time, indicating that the intracellular uptake of both SLN/Dox and Cet-SLN/Dox followed a time-dependent manner was also recorded and displayed in Fig. 3D. The body weight of mice in free Dox and SLN/Dox groups both exerted a tendency of steady decrease after different administration period, indicating that due to the tumor burden and/or side effects of Dox, either the living quality or health of mice was compromised, highlighting the importance of tumor-homing properties in in vivo application. As a proof of concept, no evident body weight decline was observed in Cet-SLN/Dox group, implying that the tumor-homing property of Cet-SLN/Dox not only increase their anti-cancer efficacy but also reduce their safety risks. Fig. 3E indicated the representative HE-stained tumor sections of different

groups. Typical tumor pathological characteristics were observed in groups injected with saline s. In contrast, cancer cell remission was observed in all Dox and/or Cetuximab containing groups. As predicted, mice administered with Cet-SLN/Dox displayed the most massive remission of cancer cells with the best anticancer ability, which was in consistent with above obtained results. All these data presented substantial evidence to prove the superior antitumor effect of Cet-SLN/Dox. Overall, the Cet-SLN/Dox had great potential as preferable tumor-targeting DDS for potential liver cancer therapy

4. Conclusion

In the present study, we successfully developed a preferable Dox loaded DDS based on Cetuximab and silica nanoparticles (Cet-SLN/ Dox). By employing the tumor homing property of Cetuximab and the drug-loading capability of silica nanoparticles, the prepared Cet-SLN/Dox was able to load Dox to achieve the co-delivery of two drugs (Cetuximab and Dox). On the other hand, the Cet-SLN/Dox was capable of releasing the loaded drugs with a redox responsive and successive manner. Both in vitro and in vivo experiments revealed that Cet-SLN/Dox had superior tumor-homing property than the Cetuximab free one (SLN/Dox). Moreover, binary DDS Cet-SLN/ Dox exhibited much more potent anti-cancer effects than the mono DDS SLN/Dox.

Declaration of competing interest

The authors declare no conflict of interest, financial or otherwise.

Acknowledgements

This research did not receive any specific grant from funding agencies in the public, commercial, or not for profit sectors. The authors are helpful to the National Institute of Technology (NIT), Rourkela, Odisha, India for providing all required facilities.

References

1. R. Lozano, M. Naghavi, K. Foreman, S. Lim, K. Shibuya, V. Aboyans, et al., Global and regional mortality from 235 causes of death for 20 age groups in 1990 and 2010: a systematic analysis for the global burden of disease study 2010, *Lancet* 380 (2013) 2095–2128.
2. R. Siegel, D. Naishadham, A. Jemal, Cancer statistics, 2012, *CA Cancer J. Clin.* 62 (2012) 10–29.
3. S. Abbad, C. Wang, A.Y. Waddad, H. Lv, J. Zhou, Preparation, in vitro and in vivo evaluation of polymeric nanoparticles based on hyaluronic acid-poly (butyl cyanoacrylate) and D-alpha-tocopheryl

- polyethylene glycol 1000 succinate for tumor-targeted delivery of morin hydrate, *Int. J. Nanomedicine* 10 (2015) 305–320.
4. Q. Guo, D. Guan, B. Dong, F. Nan, Y. Zhang, Charge-conversional binary drug delivery polymeric micelles for combined chemotherapy of cervical cancer, *Int. J. Polym. Mater. Polym. Biomater.* 64 (2015) 978–987.
5. Q. Ouyang, Z. Duan, G. Jiao, J. Lei, A biomimic reconstituted high-density lipoprotein-based drug and p53 gene co-delivery system for effective antiangiogenesis therapy of bladder cancer, *Nanoscale Res. Lett.* 10 (2015) 283.
- [6] X. Sun, W. Wang, J. Huang, H. Lai, C. Guo, C.A. Wang, A biomimic reconstituted high density lipoprotein nanosystem for enhanced VEGF gene therapy of myocardial ischemia, *J. Nanomater.* 2015 (2015) 8, 693234. <http://dx.doi.org/10.1155/2015/693234>.
7. C. Wang, X. Bao, X. Ding, Y. Ding, S. Abbad, Y. Wang, et al., A multifunctional selfdissociative polyethyleneimine derivative coating polymer for enhancing the gene transfection efficiency of DNA/polyethyleneimine polyplexes in vitro and in vivo, *Polym. Chem.* 6 (2015) 780–796.
8. H. Lu, H. Zhang, D. Zhang, H. Lu, D. Ma, A biocompatible reconstituted high-density lipoprotein nano-system as a probe for lung cancer detection, *Med. Sci. Monit.* 21 (2015) 2726–2733.
9. M. Li, Y. Li, X. Huang, X. Lu, Captopril-polyethyleneimine conjugate modified gold nanoparticles for co-delivery of drug and gene in anti-angiogenesis breast cancer therapy, *J. Biomater. Sci. Polym. Ed.* 16 (2015) 1–15.
10. H. Wu, Y. Zhao, X. Mu, H. Wu, L. Chen, W. Liu, et al., A silica–polymer composite nano system for tumor-targeted imaging and p53 gene therapy of lung cancer, *J. Biomater. Sci. Polym. Ed.* 26 (2015) 384–400.
11. E. Liu, Y. Zhou, Z. Liu, J. Li, D. Zhang, J. Chen, et al., Cisplatin loaded hyaluronic acid modified TiO₂ nanoparticles for neoadjuvant chemotherapy of ovarian cancer, *J. Nanomater.* 2015 (2015) 8, 390358. <http://dx.doi.org/10.1155/2015/390358>.
12. S. Santra, P. Zhang, K. Wang, R. Tapeç, W. Tan, Conjugation of biomolecules with luminophore-doped silica nanoparticles for photostable biomarkers, *Anal. Chem.* 73 (2001) 4988–4993.
13. I.I. Slowing, B.G. Trewyn, S. Giri, V.Y. Lin, Mesoporous silica nanoparticles for drug delivery and biosensing applications, *Adv. Funct. Mater.* 17 (2007) 1225–1236.
14. F. Tang, L. Li, D. Chen, Mesoporous silica nanoparticles: synthesis, biocompatibility and drug delivery, *Adv. Mater.* 24 (2012) 1504–1534.

15. W. He, S. Huang, C. Zhou, L. Cao, J. Yao, J. Zhou, et al., Bilayer matrix tablets for prolonged actions of metformin hydrochloride and repaglinide, *AAPS PharmSciTech* 16 (2015) 344–353.
16. K. Yu, S. Wu, H. Li, A chitosan-graft-PEI-eprosartan conjugate for cardiomyocytetargeted VEGF plasmid delivery in myocardial ischemia gene therapy, *J. Exp. Nanosci.* 1 (2015) 1–16.
17. A. Huether, M. Höpfner, V. Baradari, D. Schuppan, H. Scherübl, EGFR blockade by cetuximab alone or as combination therapy for growth control of hepatocellular cancer, *Biochem. Pharmacol.* 70 (2005) 1568–1578.
18. C. Liao, Q. Sun, B. Liang, J. Shen, X. Shuai, Targeting EGFR-overexpressing tumor cells using cetuximab-immunomicelles loaded with doxorubicin and superparamagnetic iron oxide, *Eur. J. Radiol.* 80 (2011) 699–705.
19. R.V. Kutty, S.-S. Feng, Cetuximab conjugated vitamin E TPGS micelles for targeted delivery of docetaxel for treatment of triple negative breast cancers, *Biomaterials* 34 (2013) 10160–10171.
20. M. Antonietti, R. Basten, S. Lohmann, Polymerization in microemulsions a new approach to ultrafine, highly functionalized polymer dispersions, *Macromol. Chem. Phys.* 196 (1995) 441–466.
21. A.J. Zarur, J.Y. Ying, Reverse microemulsion synthesis of nanostructured complex oxides for catalytic combustion, *Nature* 403 (2000) 65–67.
22. M. Gao, L. Sun, Z. Wang, Y. Zhao, Controlled synthesis of Ag nanoparticles with different morphologies and their antibacterial properties, *Mater. Sci. Eng., C* 33 (2013) 397–404.
23. R.V. Kutty, S.L. Chia, M.I. Setyawati, S.S. Muthu, S.S. Feng, D.T. Leong, In vivo and ex-vivo proofs of concept that cetuximab conjugated vitamin E TPGS micelles increases efficacy of delivered docetaxel against triple negative breast cancer. *BIOMATERIALS 2015*, *Biomaterials* 63 (2015) 58–69.
24. C. Berasain, L.M. Ujue, R. Urtasun, S. Goñi, M. Elizalde, O. Garciairigoyen, et al., Epidermal growth factor receptor (EGFR) crosstalks in liver cancer, *Cancer* 3 (2011) 2444–2461